

This is the peer reviewed version of the following article:

Active Safety System with RF Energy Harvesting Capabilities for Industrial Applications using Interchangeable Implements / Bertacchini, Alessandro; Napoletano, Giacomantonio; Scorcioni, Stefano; Larcher, Luca; Pavan, Paolo. - ELETTRONICO. - (2014), pp. 5286-5292. (Intervento presentato al convegno 40th Annual Conference on IEEE Industrial Electronics Society - IECON 2014 tenutosi a Dallas nel October 29 - November 1 2014) [10.1109/IECON.2014.7049307].

IEEE

Terms of use:

The terms and conditions for the reuse of this version of the manuscript are specified in the publishing policy. For all terms of use and more information see the publisher's website.

note finali coverpage

28/11/2023 11:54

(Article begins on next page)

Active Safety System with RF Energy Harvesting Capabilities for Industrial Applications using Interchangeable Implements

A. Bertacchini, S. Scorcioni, L. Larcher

Department of Engineering Sciences and Methods
DISMI -University of Modena and Reggio Emilia
Reggio Emilia, Italy
alessandro.bertacchini@unimore.it

G. Napoletano, P. Pavan

Department of Engineering "Enzo Ferrari"
DIEF -University of Modena and Reggio Emilia
Modena, Italy

Abstract—In this paper a system for the remote powering of low power electronic devices is presented. The system has been applied to a real industrial application allowing to enhance active safety in industrial vehicles. It is comprised of two main devices: i) the End Device (ED) with an embedded Radio Frequency (RF) energy harvester; ii) the Illuminator-Gateway Device (IGD) with an embedded RF power transmitter. Thanks to the optimization of the customized dual band Planar Inverted Folded Antenna (PIFA) used, the ULP architecture of the ED, the hardware-software co-design approach used and the optimization of the ED firmware, the proposed system is able to provide up to the 63% of the power required by the ED when it is on duty.

Keywords—RF power delivery, RF energy harvesting, Low Power Electronics, HW/SW Codesign, Active Safety

I. INTRODUCTION

Nowadays the safety is a mandatory requirement in a growing number of industrial applications and new safety functions can be added to existing systems in several ways. One of the most investigated solution is the use of Ultra Low Power (ULP) Wireless Sensor Node (WSN). Currently, batteries are used to power supply this kind of devices, but despite the continuous power consumption reduction of commercial hardware components, the limited lifetime of the batteries is still one of the limiting factors to the extensive use of WSN. Moreover batteries have an high environmental impact and high maintenance costs (e.g. replacement or recharge), especially in case of high density sensor networks. Consequently there is an increasing interest in the study of alternative energy sources.

Even though the availability of energy strongly depends on the environment where the devices work, alternative power supply solutions based on energy harvesting systems have been proposed. In order to alleviate this issue, remote power delivery systems exploiting ad-hoc generated RF signals have been investigated. But these solutions have to deal with the very low amount of power available at far locations and the unpredictable variations of available power due to several factors like the distance from the power source and the antenna orientation.

Several papers have been presented covering the topic of efficient RF-DC power converters, e.g. [1]. Most of them aimed only at maximizing the circuit efficiency at a given input power level, e.g. [2]-[3], while neglecting the issues related to input power variations.

The RF power delivery system proposed in this paper aims to overcome these limitations considering also other typical boundary conditions of real industrial scenarios like systems with more than one degree of freedom (e.g. robotic arms, manipulators, car transportations systems, earthmoving machineries or telehandlers). In particular, the distance and the alignment between transmitter and receiver may vary significantly during the normal operation, affecting the amount of energy effectively delivered and the overall system efficiency.

The paper is organized as follows. Section II describes the proposed system architecture. Section III presents the main characteristics of the implemented communication protocol. Experimental results are shown in Section IV, while Section V concludes the paper.

II. SYSTEM ARCHITECTURE

The proposed RF power delivery system can be used in several industrial applications. The considered case study concerns the active safety enhancement in telehandlers, thanks to the automatic identification of the implements connected to the telescopic arm of the vehicle.

As shown in Fig. 1, the system is comprised of two main devices: the Illuminator-Gateway Device (IGD), mounted on the free end of the telescopic arm of the telehandler, and the End Device (ED), mounted on the connected implement. Data between IGD and ED are exchanged exploiting a 2.4GHz bidirectional wireless link, while the RF power delivery system exploits two customized dual band Planar Inverted Folded Antenna (PIFA) optimized to work at both 869 MHz and 915 MHz. The implemented prototypes are shown in Fig.2.

The IGD has two functions: i) operates as gateway for data exchange between ED and the Electronic Control Units (ECUs) of the vehicle by means of a standard CANopen

communication; ii) once the association with the ED is established, the IGD generates the RF power signal used for the remote powering of the ED. The transmitted RF signal is compliant with both the regulations in force in EU and North America.

The ED embeds an RF energy harvesting circuit that collects and converts the RF energy delivered by the IGD. The energy gathered by the harvester is handled by a power management circuit that supplies the ED during its normal operation, and recharges a Li-Ion backup battery in case of surplus of incoming RF energy.

The parameters of the implement are preloaded in the ED at programming time. When the implement is physically connected with the telehandler, the ED requests a connection with the IGD, which can be completed only if the ED is compatible with the IGD. After that, the ED can start the computation of the effective implement working time, which is used by the IGD for programmed maintenance purposes.

The actual working condition of the ED is determined by two concurrent events: i) the presence of vibrations on the ED, detected by means of a 3D accelerometer integrated on the device; ii) an IGD-ED association is established.

In the considered application the relative positioning between ED and IGD can vary in a no predictable way. In fact, when a telehandler is on duty, the extension and the working height of its telescopic arm can change continuously depending on the current working task, and the implement have to rotate in order to obtain the optimal working position. The rotation of the implement causes a variation of both relative distance and relative orientation between IGD (i.e. RF power transmitter) and ED (i.e. RF power harvester), which needs to be taken into account at the design phase. In the same way, the use of a customized antenna designed to work efficiently in condition of no/poor alignment between transmitter and receiver, the materials of the housing and the fixing brackets of the devices have to be taken into account, at the design phase to improve the performance of the whole system.

A. Illuminator-Gateway Device (IGD) with embedded RF Power Transmitter

A simplified block diagram of the IGD is shown in Fig. 1. The core of the IGD hardware architecture is a Texas Instruments ARM Cortex-R microcontroller with a dual core lock-step CPU, clock frequency up to 220 MHz, single bit error correction and double bit error detection. The IGD has been designed to be compliant with the IEC 61508 regulation and to guarantee high performances in terms of real-time execution and fault tolerance. This redundant architecture allows to inform the operator and any other electronics on board about detected failures leading to potentially dangerous situations for the safety of both machine and operator (e.g. memory overwriting, clock fault or disagreement in computations of the two CPU).

The IGD has two main tasks. The first one is to operate as gateway in the data exchange between the ED and any other electronic devices on board (e.g. other ECUs). It uses a 2.4GHz wireless protocol to communicate with the ED, while it

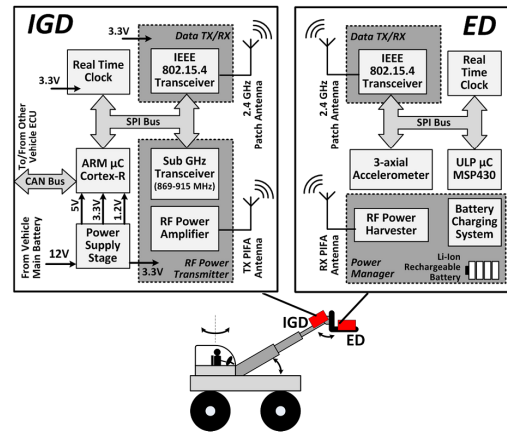


Fig. 1. Simplified block diagram of the proposed remote power delivery system with the main functional blocks of IGD and ED highlighted.

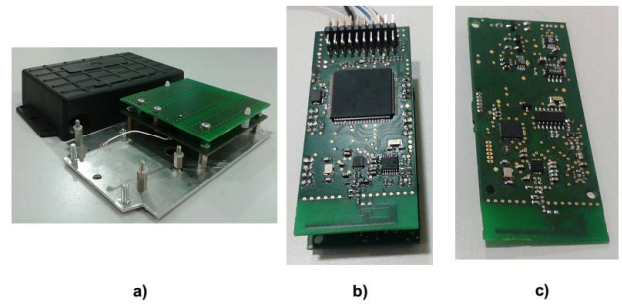


Fig. 2. Implemented prototypes. a) PIFA with aluminum cover and plastic housing. Two prototypes have been realized. The first one is used for the IGD, the second one is used for the ED. The free space is reserved for the electronic circuitry (ED or IGD); b) IGD prototype; c) ED prototype.

exploits a 250 Kbps CANopen based protocol to communicate with any other ECU on the vehicle. The wireless communication between IGD and ED is implemented using a 2.4GHz low-power and IEEE 802.15.4 compliant transceiver (i.e. CC2500 from Texas instruments), and a customized patch antenna.

The implement parameters received from the ED are used to check if the implement is compatible with the telehandler on which the IGD is mounted. If there is a positive match, the IGD executes the linking procedure with the ED and the normal operation of the system can start. Vice versa, the linking procedure is aborted and the operator is warned about a potentially dangerous working condition derived from the use of a not compatible implement. Moreover, according to the effective working time of the implement received from the ED, the IGD warns about the need of maintenance of the connected implement. The Real Time Clock (RTC) integrated in the IGD is used for the consistency check of both counter and calendar data sent by the ED.

The second task of the IGD is the generation of the RF signal used to deliver the RF power to the ED. The implemented system is compliant with both the regulations in force in Europe (ETSI 300-220, [4]) and North America (FCC part 15.247, [5]). To obtain the compliance, the IGD exploits the same hardware architecture for both the regulations, and only slight modifications in the value of passive RF

components and in the firmware (e.g. to set the desired carrier frequency which is different for the two regulations) are needed. The RF power signals delivered to the ED is generated by a sub-GHz transceiver (i.e. CC1120 from Texas Instruments), which is controlled by the microcontroller through a classic SPI communication. Depending on the regulation, the carrier frequency of the generated signal is 869.525 MHz for EU or 915 MHz with Frequency-Hopping Spread Spectrum (FHSS) algorithm for North America. In both cases the CC1120 output narrowband single-tone signals have been generated by configuring the transceiver in continuous transmission mode. The signals have been amplified up to +26 dBm exploiting a CC1190 range extender from Texas Instruments. The implemented FHSS algorithm uses 50 channels in the 914-916 MHz range, with a channel spacing of 40 KHz and dwell time of 400 ms for each channel.

In order to avoid useless transmissions, the RF power transmission starts only when an ED is detected and associated with the IGD and ends once the ED is disconnected.

B. End Device (ED) with RF Power Harvester and Power Management Policy

A simplified block diagram of the realized ED is shown in Fig. 1. The ED embeds a Texas Instruments MSP430F2274 ULP microcontroller, while the wireless communication with the IGD exploits the same hardware architecture described for the IGD, i.e. CC2500 2.4GHz transceiver with dedicated patch antenna.

The ED is in charge to count the effective working time of the implement on which it is mounted. It uses a Microchip MCP795W21 ULP Real Time Clock (RTC), which communicates with the microcontroller sharing a classic SPI bus with the wireless transceiver and a STMicroelectronics LIS3DH ULP 3-axial accelerometer. The accelerometer is periodically waked up by the microcontroller to check the presence of vibrations. If vibrations higher than 50mg are detected in at least one axis of the accelerometer, the ED starts the linking procedure described in Section III.

The ED embeds also the customized power management circuit shown in Fig. 3. The circuit is comprised of a RF energy harvester based on a commercial RF-DC converter (i.e. P2110 from Powercast) and a battery charger (i.e. LTC4070 from Linear Technology). The RF-DC converter is comprised of two main functional blocks: a voltage rectifier used to charge the external capacitor C_{STORE} by means of the harvested RF energy, and an output DC-DC converter exploiting the energy stored in C_{STORE} to provide a regulated DC voltage. In order to ensure the service continuity also in case of no/few RF energy gathered by the harvester (e.g. due to a prolonged unfavourable relative positioning between ED and IGD), a rechargeable Li-Ion battery is added to the power supply stage of the ED. The implemented power manager has been designed to efficiently combine the RF energy harvested with the energy provided by battery. Depending on both the instantaneous amount of collected RF energy and the instantaneous energy requirements of the ED, the power management circuit exploits directly the RF energy harvested, or the energy stored in the battery, or both to power supply the ED. If the collected energy is higher

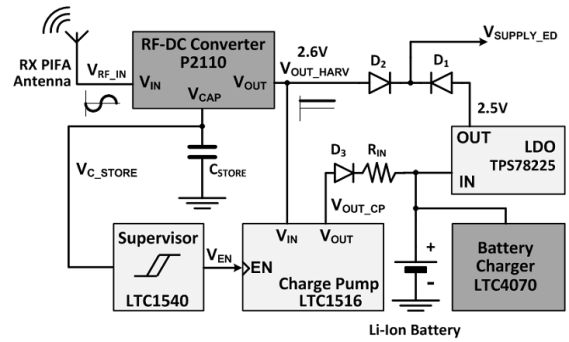


Fig. 3. Simplified block diagram of the ED power management circuit with main functional blocks highlighted.

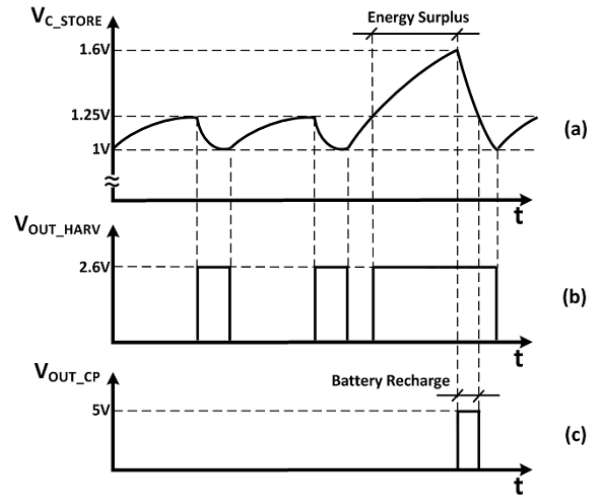


Fig. 4. Qualitative schematization of the basic operating principle of the implemented power management system through key waveforms (time axis not in scale). a) Voltage across C_{STORE} ; b) RF-DC converter output voltage; c) Charge pump output voltage.

than the energy required by the ED, the exceeding energy is used to recharge the battery.

The operating principle of the system can be understood by considering the waveforms of the signals shown in Fig. 4.

Under the assumption that the ED is in the working range of the IGD (i.e. a significant amount of RF energy is captured by the implemented RF antenna) and a RF power transmission is in progress, the voltage across C_{STORE} , i.e. V_{C_STORE} , rises. Until $V_{C_STORE} \leq 1.25$ V, the output of the RF-DC converter is disabled and the ED is powered by the back-up battery through the TPS78225 2.5V Low Drop-Out (LDO) regulator from Texas Instruments.

This condition occurs after a long time of inactivity of the implement on which the ED is mounted, or when, at a given instant, the energy requirement of the ED is much more higher than the amount of the energy harvested and stored in C_{STORE} .

Once V_{C_STORE} reaches 1.25V, the output of the RF-DC converter, is enabled and its output voltage V_{OUT_HARV} is set to 2.6V. Thanks to the diodes D_1 and D_2 , the ED is thus powered by the energy stored in C_{STORE} . If there is no RF power

transmission in progress, or the energy requirement of the ED is higher than the amount of collected RF energy, V_{C_STORE} decreases.

When $V_{C_STORE} = 1V$, the output of the RF-DC converter is disabled and the ED is powered again by the battery. Of course V_{C_STORE} decreases quickly if the energy mismatch between required and total available energy is large. If the harvested RF energy is larger than the energy required by the ED to execute its current task, V_{C_STORE} continues to rise above 1.25V, and the energy in excess is used to recharge the battery through the implemented battery charging circuit. The average charging current, I_{CHG_AVG} , is defined by the input resistance of the battery charger, R_{IN} , according to (1)

$$I_{CHG_AVG} = \frac{V_{OUT_CP} - V_{BAT}}{R_{IN}} \quad (1)$$

where $V_{OUT_CP} = 5V$ is the output voltage of the charge pump (i.e. LTC1516 from Linear Technology) used to boost the output voltage of the RF-DC converter, and $V_{BAT} = 3.7V$ is the nominal voltage of the battery. For the considered case study $I_{CHG_AVG} = 2.7mA$, with $R_{IN} = 470\Omega$.

The charge pump is enabled by means of a supervisor circuit based on the LTC1540 ULP hysteresis comparator from Linear Technology. The supervisor continuously checks V_{C_STORE} , and enables the charge pumping circuit when $V_{C_STORE} = 1.6V$. This value has been chosen according to the specifications of the commercial P2110 RF-DC converter used.

V_{C_STORE} decreases during the battery recharge and when $V_{C_STORE} = 1.25V$ the exceeding energy has been completely used. The charge pump is disabled, while the output of the RF-DC converter, V_{OUT_HARV} , is enabled until V_{C_STORE} reaches the lower bound (i.e. 1V) continuing to provide energy to the ED.

C. Planar Inverted Folded Antenna - PIFA

The RF power link exploits the same antenna for both IGD and ED. It is a customized dual band Planar Inverted Folded Antenna (PIFA). It has been optimized to operate at the frequencies of 869 MHz and 915 MHz, according to the regulations in force in Europe [4], and North America [5]. As shown in Fig. 2a, the PIFA consists of a ground plane connected with a top plate element by means of a feed wire and one or more shorting elements. The PIFA solution has the advantages of reduced sizes, large bandwidth and high antenna gain [6]. As demonstrated in [7]-[8], additional resonance frequencies can be easily obtained adding parasitic elements (patches) to the main patch of the top plate. The tuning of the desired resonance frequencies can be obtained changing: i) the distance between top plate and ground plane, ii) the dimensions and the relative positions of the parasitic elements on the top plate, iii) the position of feed wire and shorts on the top plate, iv) the dielectric constant of the substrate.

The effects of variation in the antenna directivity and asymmetries in the radiation diagram due to the parasitic elements of the PIFAs are usually undesired. In the proposed antenna solution they are exploited to improve the power link efficiency in case of no/poor alignment between transmitting and receiving antenna.

The designed PIFA antennas have a square footprint of 79 x 79mm and has been implemented using a commercial double side 1.6mm thick FR4 substrate with copper thickness of 35µm on each side. The distance between ground plane and top plate, H , is 8 mm, while the distance between the ground plane and aluminium cover of the plastic housing, H_{al} , is 12mm. The choice of H and H_{al} is a trade-off between the bandwidth at the target frequencies and physical dimensions of the PIFA. The shorting elements have been realized using commercial braces of brass. The brass feed has a diameter of 1.02 mm. The optimal values of all the design parameters (i.e. dimension and relative positioning of patches, shorts and feed wire) have been obtained from a parametric optimization carried out using a commercial electromagnetic simulator.

Experimental results not reported in detail for brevity, show that both the implemented PIFAs show a reflection coefficient lower than -20 dB at both the frequencies of interest. The measured bandwidth, calculated for a VSWR of 2:1, is 10 MHz at 869 MHz and 25 MHz at 915 MHz, while the antenna gain is higher than 0 dBi at 869 MHz and higher than +1dBi at 915 MHz for a wide span of radiation angle, peaking at +2 dBi and +4 dBi, respectively.

III. COMMUNICATION PROTOCOL

The wireless data exchange between ED and IGD has been realized by means of a communication protocol based on three main functional modes: Parking Mode, Advertising Mode and Link Mode. The simplified sequence diagram of Fig. 5 shows all the activities required to establish a correct communication.

During the inactivity period of the implement on which the ED is mounted, the ED is in Parking Mode (PM). The microcontroller is in deep-sleep mode and all the peripherals are turned off with the exception of the RTC. The RTC awakes periodically the microcontroller every ED_Park_Sleep seconds. The generated interrupt is used to turn on the accelerometer which measures the 3-axial accelerations for approximately 1.3 seconds at a sampling rate of 100Hz.

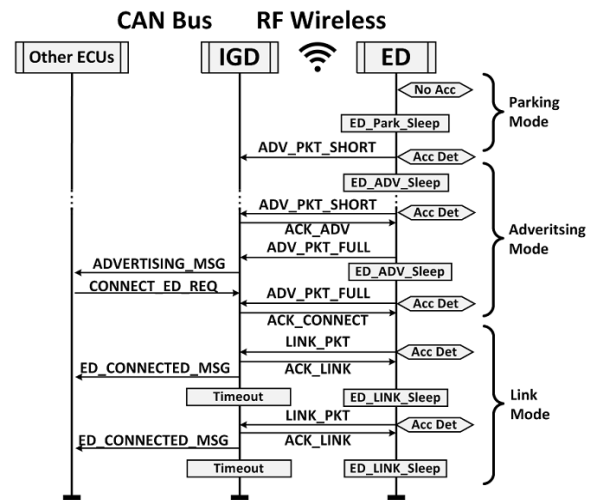


Fig. 5. Chronological sequence of messages exchanged among ED, IGD and other vehicle ECU with ED operational mode highlighted.

If at least one of the measured accelerations is higher than 50mg, then a potential working condition occurs and the ED enter in Advertising Mode (ADVM).

When in Advertising Mode, the ED transmits a wireless Advertising Packet (ADV_PKT_SHORT) every ED_ADV_Sleep seconds. The packet contains its unique identifier and a minimal set of parameters identifying the implement. If no acknowledgment from the IGD is received after the transmission of the third ADV_PKT_SHORT the ED goes again in Parking Mode. Vice versa if an IGD responds by sending an Acknowledgment Packet (ACK_ADV) the ED sends a full advertising packet (ADV_PKT_FULL) containing the full set of the implement parameter (barycenter, weight, load capacity, etc...) and the connection procedure continues. The IGD forwards the notification of the connection request (ADVERTISING_MSG) coming from the ED to the ECU where the stability control algorithms of the vehicle run.

The ECU checks if the implement associated with the ED is compatible with the vehicle and if there is any other connection procedure ongoing. If these checks are passed, the ECU sends to the IGD a CAN message (CONNECT_ED_REQ) containing the unique identifier of the ED.

At this time, when another ADV_PKT_FULL with the specified identifier is received from the ED, the IGD in turn sends a wireless packet (ACK_CONNECT) confirming its availability to continue the linking procedure. The ED replies by sending the Link packet (LINK_PKT) to the IGD and switches in Link Mode (LM). Any other connection request coming from other EDs is discarded by the IGD (for safety reasons, only one ED at a time can be linked with the IGD).

Once in Link Mode, the ED starts the count of the effective working time of the implement. The count is updated every ED_Link_Sleep seconds, which is the time interval occurring between two consecutive transmissions of LINK_PKT from the ED to the IGD. The function of the LINK_PKT is twofold. First, the information contained in it are forwarded to other vehicle ECUs via CAN messages (ED_CONNECTED_MSG) for continuous consistency checks between the implement on duty and the current operation requested by the operator. Second, the LINK_PKT are used as “*alive messages*” to check if the ED is working properly. Whenever a LINK_PKT is received the IGD sends an acknowledgement message (ACK_LINK) to the ED. If the ED does not receive any ACK_LINK within a defined timeout, it comes back in Parking Mode. If the IGD does not receive any LINK_PKT within a defined timeout, it sends a dedicated CAN message to the other ECUs to notify the disconnection of the implement and of its ED.

Under the reasonable assumption that vibrations occur on the implement when it is on duty, accelerations are periodically checked by the ED in order to verify the effective working condition of the implement. If no vibrations are detected for three consecutive samples the ED does not send more LINK_PKT and the disconnection procedure starts.

In ULP wireless devices the highest power consumption occurs during the data transmission [9]. At the same time, it is fundamental to minimize the device power consumption when

in idle state, because lower is the duty cycle higher is the percentage of the device power consumption due to this state. With respect to these general design guidelines the implemented ED exploited an hardware-software co-design approach to minimize its power consumption. The system resources (e.g. microcontroller peripherals, accelerometer, RF transceiver, etc...) are enabled only for the time required to execute their tasks, being completely turned off for the rest of the time.

From the point of view of the communication protocol, the main efforts have been devoted to the minimization of both the overall time needed to establish the connection between IGD and ED, and the transmission/reception time of the exchanged data packets. Considering the connection procedure described above, the Advertising Mode is the most power consuming phase. Since the IGD has no power consumption constraints, it is always on. To shorten the ED_ADV_Sleep time allows to shorten the overall connection procedure time. At the same time the data packets length has been modulated according to the current phase of the Advertising Mode. In particular, the ADV_PKT_SHORT is used in the first part of the Advertising Mode when the ED has detected vibrations but it does not know if there is an IGD in its operating range. In this condition the ED sends a reduced data packet of 13 bytes containing only the unique identifier of the ED, the ED status and the working time counters. The ADV_PKT_FULL, instead, has a length of a 52 bytes. It contains the complete set of implement parameters and it is sent only in the second part of the Advertising Mode to complete the connection procedure (i.e. after that the ED has received the acknowledgment packet ACK_ADV from the IGD).

In Link Mode, the framework of the transmitted LINK_PKT is similar to the ADV_PKT_SHORT one. In fact, the ED and the relative implement have been completely identified during the Advertising Mode, and there is no need to transmit the full set of implement parameters which is a very time and power consuming task.

IV. EXPERIMENTAL RESULTS

The system has been characterized by evaluating both the ED power consumption in every operational mode and its self-sustainability in terms of energy harvesting capabilities when in normal working conditions (i.e. Link Mode).

A. ED Characterization

The ED current consumption was measured for every operating mode of the device (Parking Mode, Advertising Mode and Linked Mode). The measurements were carried out by means of a N6784A battery drain module integrated into N6705B DC power analyzer from Agilent Technologies with dedicated 14585A Analysis Software.

When the ED is in Parking Mode (see Fig. 6), it remains in deep sleep for the most of the time with an average current consumption of 5 μ A, mainly due to the current consumption of the RTC. The ED wakes up every $ED_Park_Sleep = 30$ sec to check the presence of vibrations. The measurement lasts approximately 1.3 sec with an average current consumption of 15 μ A, peaking up to 300 μ A during the 10 msec of the

accelerometer awaking. With the chosen ED_Park_Sleep time interval, the total average current consumption of the ED in Parking Mode, $I_{ED_Park_avg}$, is $\sim 5.5 \mu A$.

In Advertising Mode, the ED wakes up from the sleep mode (i.e. $5 \mu A$ of average ED current consumption) every $ED_ADV_Sleep = 5$ sec in order to check the presence of an IGD. In the first part of the Advertising Mode the ED sends an ADV_PKT_SHORT data packet containing only the basic parameters of the associated implement. The relative ED current consumption profile is shown in Fig. 7a. The data transmission and its related computations lasts approximately 40 msec with an average current consumption of 17mA, peaking up to 23mA. With the considered ED_ADV_Sleep time interval the average current consumption of the ED is $\sim 140 \mu A$.

In the second part of the Advertising Mode, the ED sends an ADV_PKT_FULL containing all the parameters of the implement on which the ED is mounted (see Fig. 7b). The total task duration lasts approximately 90msec with an average current consumption of approximately 17mA.

In Link Mode the ED sends a LINK_PKT with the same framework of the ADV_PKT_SHORT every $ED_Link_Sleep = 58$ sec with the message fields reserved for the effective working time count updated at each transmission. The ED current consumption is consequently the same one described for the first stage of the Advertising Mode (see Fig. 7a). Of course, the average current consumption in Link Mode, $I_{ED_Link_avg}$, drops significantly to $17 \mu A$, due to the longest sleeping time between two consecutive data transmissions.

The time intervals ED_Park_Sleep , ED_Link_Sleep and ED_ADV_Sleep can be set at programming time and have to be chosen as a tradeoff between the timing requirements of the specific application and the minimization of the ED power consumption.

B. RF Energy Harvester Characterization

The measured current consumption of the ED allowed to estimate the average contribution of the implemented RF energy harvester to the self-sustainability of the ED. It can be expressed as ratio between the average current provided from the RF energy harvester and the average current required by the ED for its proper operation.

To estimate the amount of power effectively delivered to the ED three main factors must be taken into account: i) the ED power consumption varies significantly depending on the operational mode; ii) the IGD cannot provide RF power continuously due to the regulations currently in force; iii) the amount of harvested RF power is not constant because it depends on the distance between IGD and ED and on their relative alignment, which vary significantly during the normal working conditions of the implement.

The characterization of the RF energy harvester has been carried out measuring the average percentage of self-sustainability of the ED when it works in Link Mode. Indeed, the Link Mode is the only operational mode where the IGD delivers RF power to the ED. Moreover, it is reasonable to assume that the ED operates in Link Mode for the most of the time.

The measurements have been carried out using the setup sketched in Fig. 8. The characterization setup has been developed to simulate the misalignment between ED and IGD occurring during the normal operation of the implement connected to the telescopic arm of the telehandler. The IGD has been kept in a fixed position while the ED has been positioned at different distances d and angles θ_1 from the IGD. For each relative position, identified by (d, θ_1) , three different measurements have been performed rotating the ED around its vertical axes with angles θ_2 .

The ED power requirements at a given time are strongly dependent on the instantaneous task in execution and the equivalent resistance at the output of the harvester ranges from $k\Omega$ (e.g. when ED transmits to IGD) to hundreds of $k\Omega$ (e.g. when ED is in sleep mode).

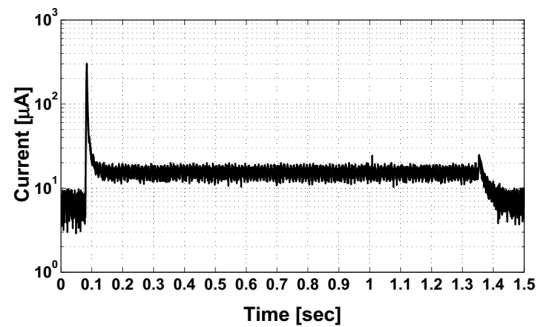


Fig. 6. Current consumption of the ED when in Parking Mode.

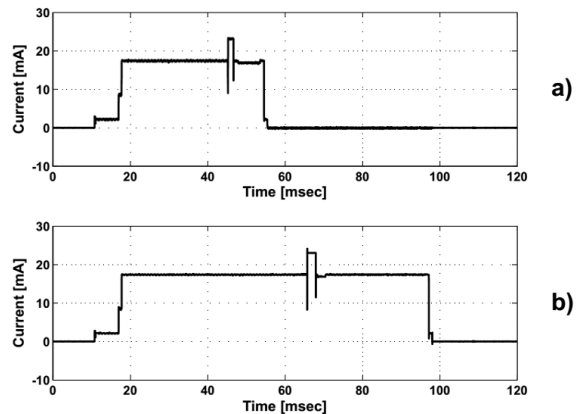


Fig. 7. Current consumption of the ED when in Advertising and Link Mode. a) Current profile of the transmission of ADV_PKT_SHORT and LINK_PKT during the first stage of the advertising mode and the normal operation in Link Mode; b) Current profile of the transmission of ADV_PKT_FULL during the final stage of the connection procedure in Advertising Mode.

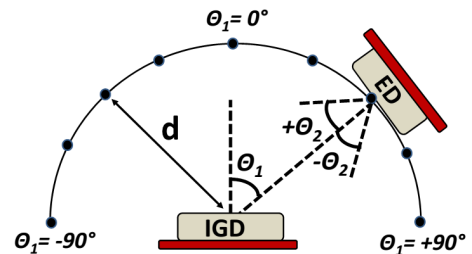


Fig. 8. Setup used for the RF energy harvester characterization.

In Link Mode, the measured average current consumption of the ED is $I_{ED_Link_avg} = 17 \mu A$, while the regulated output voltage of the DC-DC converter embedded in the commercial P2110 RF harvester used is 2.6V. The ED power consumption is hence represented by the equivalent load resistance $R_{Load} = 2.6V/17\mu A \approx 150k\Omega$. The efficiency of the P2110 output DC-DC converter used, η_{DC-DC} , has been separately characterized for different values of R_{Load} . Obtained results shown that it ranges from 27% to 66%, according to the applied load. In particular, at the working conditions of the ED when in Link Mode (i.e. $R_{Load} = 150k\Omega$) corresponds a DC-DC efficiency $\eta_{DC-DC} = 45\%$, which strongly affects the overall system efficiency.

Using this efficiency value and measuring the time t_{chrg} needed to charge the 1mF storage capacitor C_{STORE} , the self-sustainability of the ED has been evaluated by calculating the average current available at the output of the RF energy harvester, I_{Harv_avg} , using (2)

$$I_{Harv_avg} = \frac{1}{2} C_{STORE} (V_{CS_H}^2 - V_{CS_L}^2) \frac{1}{t_{chrg}} \frac{1}{V_{out_harv}} \eta_{DC-DC} \quad (2)$$

where $V_{CS_L} = 1V$ and $V_{CS_H} = 1.25V$ are respectively the start-charge and end-charge threshold voltages of C_{STORE} , imposed by the P2110 RF harvester on C_{STORE} during its normal operation mode, while $V_{out_harv} = 2.6V$ is the DC-DC regulated output voltage of the RF harvester used.

Exploiting the measured average current consumption of the ED in Link Mode, $I_{ED_Link_avg}$, and the calculated I_{Harv_avg} it is easy to calculate the percentage of self-sustainability of the ED, S_{ED} , using (3)

$$S_{ED} [\%] = 100 \frac{I_{Harv_avg}}{I_{ED_Link_avg}} \quad (3)$$

The results in case of RF signals compliant with the EU regulation are reported in Table I. The implemented RF energy harvesting system provides a significant amount of energy to the ED in a wide range of configurations (d , θ_1 , θ_2). In particular, when the optimal relative positioning between IGD and ED occurs, up to the 63% of the average power required by the ED in Link Mode is provided by the realized RF harvester. Finally, as reported in Table I, not all the configurations allow to deliver a significant amount of RF power to increase the lifetime of the ED battery. This is due to the cross polarization effects of the two PIFA antennas embedded in the IGD and in the ED respectively. Similar results have been obtained also in the case of IGD configured to deliver RF power at the frequency of 915MHz.

V. CONCLUSIONS

In this paper, a system for the active safety enhancement of industrial vehicles with remote RF powering of wireless sensor nodes is presented. The system has been optimized to work in conditions of poor alignment between transmitter and receiver,

TABLE I. PERCENTAGE OF SELF-SUSTAINABILITY S_{ED} OF THE ED WHEN IN LINK MODE FOR DIFFERENT RELATIVE POSITIONS BETWEEN IGD AND ED

		Distance between IGD and ED					
		$d = 35cm$			$d = 50cm$		
		θ_2 [deg]	-45	0	+45	-45	0
θ_1 [deg]	-90	N/A ^a	17.30	25.99	N/A ^a	N/A ^a	13.29
	-67.5	7.99	24.87	50.71	7.91	4.07	25.86
	-45	14.63	37.85	62.93	3.01	12.32	23.74
	-22.5	5.65	31.09	60.04	13.22	12.93	32.85
	0	13.71	23.53	45.82	3.17	4.08	17.83
	+22.5	20.81	16.37	23.32	13.60	N/A ^a	8.11
	+45	15.97	9.12	5.42	N/A ^a	N/A ^a	N/A ^a
	+67.5	10.08	N/A ^a				
	+90	N/A ^a	N/A ^a	N/A ^a	N/A ^a	N/A ^a	N/A ^a

^a: N/A = $S_{ED} < 3\%$

which is a typical working conditions of systems with more than one degree of freedom.

The antenna optimization, the ULP architecture and the hardware-software co-design approach used, allowed to implement a RF harvester able to generate up to the 63% of the power required by the ED when in Link Mode (i.e. when the implement is on duty) and the optimal relative positioning between IGD and ED occurs. In other configurations the lifetime of the ED battery is extended according to the presented results.

REFERENCES

- [1] S. Scorcioni, A. Bertacchini, L. Larcher; "A 868MHz CMOS RF-DC power converter with $-17dBm$ input power sensitivity and efficiency higher than 40% over 14dB input power range" in *Proc. Int. Conf. on European Solid Stat Circuits*, Sept 2012, Vol. 1, pp.109-112.
- [2] J.-P. Curty, N. Joehl, F. Krummenacher, C. Dehollain and M.J. Declercq, "A Model for μ -Power Rectifier Analysis and Design", *Circuit and Systems I, IEEE Transactions on*, vol. 52, pp. 2771-2779, December 2005.
- [3] R.E. Barnett, Liu Jin and S. Lazar, "A RF to DC Voltage Conversion Model for Multi-Stage Rectifiers in UHF RFID Transponders," *Solid-State Circuits, IEEE Journal of*, vol.44, pp.354-370, February 2009.
- [4] ETSI EN 300 220-1 (V2.4.1), "Electromagnetic compatibility and Radio spectrum Matters (ERM); Short Range Devices (SRD); Radio equipment to be used in the 25 MHz to 1000 MHz frequency range with power levels ranging up to 500 mW", available at <http://www.etsi.org>
- [5] FCC, "§15.247 Operation within the bands 902-928 MHz, 2400-2483.5 MHz, and 5725-5850 MHz", Available: <http://www.ecfr.gov/>
- [6] K.L. Virga, Y. Rahmat-Samii "Low-profile enhanced-bandwidth PIFA antennas for wireless communications packaging", in *IEEE Trans. Microw. Theory Tech*, 1997, volume 45, issue 10, pp.1879-1888.
- [7] H.T. Chattha, Y. Huang, Y. Lu, X. Zhu; "Further bandwidth enhancement of PIFA by adding a parasitic element", in *Proc. Int. Conf. Antennas & Propagation*, 2009, Vol. 1, pp.213-216.
- [8] K. Dong-Yeon, J.W Lee, C. Choon-Sik, K. Jaeheung; "A Compact Tri-Band PIFA with Multiple-Folded Parasitic Elements", *Proc. Int. Microw. Symp. IEEE/MTT-S*, 2007, Vol. 1, pp.259-262
- [9] J. Song, Y. Kheng Tan; "Energy consumption analysis of ZigBee-based energy harvesting wireless sensor networks," in *Proc. Communication Systems (ICCS)*, 2012 IEEE International Conference on, Singapore, 2012, pp. 468-472.